

---

# EGRU: Event-based GRU for activity-sparse inference and learning

---

Anonymous Author(s)

Affiliation

Address

email

## Abstract

1 The scalability of recurrent neural networks (RNNs) is hindered by the sequential  
2 dependence of each time step’s computation on the previous time step’s output.  
3 Therefore, one way to speed up and scale RNNs is to reduce the computation  
4 required at each time step independent of model size and task. In this paper, we  
5 propose a model that reformulates Gated Recurrent Units (GRU) as an event-based  
6 activity-sparse model that we call the Event-based GRU (EGRU), where units  
7 compute updates only on receipt of input events (event-based) from other units.  
8 When combined with having only a small fraction of the units active at a time  
9 (activity-sparse), this model has the potential to be vastly more compute efficient  
10 than current RNNs. Notably, activity-sparsity in our model also translates into sparse  
11 parameter updates during gradient descent, extending this compute efficiency to  
12 the training phase. We show that the EGRU demonstrates competitive performance  
13 compared to state-of-the-art recurrent network models in real-world tasks, including  
14 language modeling while maintaining high activity sparsity naturally during  
15 inference and training. This sets the stage for the next generation of recurrent  
16 networks that are scalable and more suitable for novel neuromorphic hardware.

## 17 1 Introduction

18 Large scale models such as GPT-3 [8], switch transformers [17] and DALL-E [52] have demonstrated  
19 that scaling up deep learning models to billions of parameters cannot just improve the performance  
20 of these models but lead to entirely new forms of generalisation. For example, GPT-3 can do  
21 basic translation and addition even though it was trained only on next word prediction. While it is  
22 unknown if scaling up recurrent neural networks can lead to similar forms of generalisation, the  
23 limitations on scaling them up preclude studying this possibility. The dependence of each time step’s  
24 computation on the previous time step’s output is the source of a significant computational bottleneck,  
25 preventing RNNs from scaling well. Therefore, in recent years, RNNs, despite their many desirable  
26 theoretical properties [15] such as the ability to process much longer context and their computational  
27 power [57, 60], have been supplanted by feedforward network architectures.

28 By reducing the computation required at each time step, independent of model size and task, we can  
29 speed up and better scale RNNs. We propose to do this by designing a general-purpose event-based  
30 recurrent network architecture that is naturally activity-sparse. Dubbed the Event-based Gated  
31 Recurrent Unit (EGRU), our model is an extension of the Gated Recurrent Unit (GRU) [12]. With  
32 event-based communication, units in the model can decide when to send updates to other units, which  
33 then trigger the update of receiving units. Therefore, network updates are only performed at specific,  
34 dynamically determined event times. With activity-sparsity, most units do not send updates to other  
35 units most of the time, leading to substantial computational savings during training and inference.  
36 We formulate the gradient updates of the network to be sparse using a novel method, extending the  
37 benefit of the computational savings to training time.

38 The biological brain, which relies heavily on recurrent architectures and is at the same time extremely  
39 energy efficient [43], is a major source of inspiration for the EGRU. One of the brain’s strategies  
40 to reach these high levels of efficiency is activity-sparsity. In the brain, (asynchronous) event-based  
41 communication is just the result of the properties of the specific physical and biological substrate on  
42 which the brain is built. Biologically realistic spiking neural networks and neuromorphic hardware also  
43 aim to use these principles to build energy-efficient software and hardware models [53, 58]. However,  
44 despite progress in recent years, their task performance has been relatively limited for real-world tasks  
45 compared to state-of-the-art recurrent architectures based on LSTM and GRU. We view the EGRU as  
46 a generalisation of spiking neural networks, moving away from modeling biological dynamics toward  
47 a more general-purpose recurrent model for deep learning.

48 In this paper, we first introduce a version of EGRU based on a principled mathematical approach that for-  
49 mulates the dynamics of the internal states of the network in continuous time. The units of the network  
50 communicate solely through message events triggered when the internal state of a unit reaches a thresh-  
51 old value. This allows us to derive exact gradient descent update equations for the network analogous  
52 to backpropagation-through-time (BPTT) that mirrors the activity-sparsity of the forward pass.

53 We then introduce a discrete simplification of this continuous-time model that is also event-based  
54 and activity-sparse while being easier to implement on today’s prevailing machine learning libraries  
55 and thus directly comparable to existing implementations of GRU and LSTM. The backwards pass  
56 here uses an approximate version of BPTT, and these updates are also sparse.

57 The sparsity of the backward-pass overcomes one of the major roadblocks in using large recurrent  
58 models, which is having enough computational resources to train them. We demonstrate the task  
59 performance and activity sparsity of the model implemented in PyTorch, but this formulation will  
60 also allow the model to run efficiently on off-the-shelf hardware, including CPU-based nodes  
61 when implemented using appropriate software paradigms. Moreover, an implementation on novel  
62 neuromorphic hardware like [13, 27], that is geared towards event-based computation, can make the  
63 model orders of magnitude more energy efficient [48].

64 In summary, the main contributions of this paper are the following:

- 65 1. We introduce the EGRU, an event-based continuous-time variant of the GRU model.
- 66 2. We derive an event-based form of the error-back-propagation algorithm for EGRU.
- 67 3. We introduce a discrete-time version of EGRU that can be directly compared to current  
68 LSTM/GRU implementations.
- 69 4. We demonstrate that the EGRU exhibits task-performance competitive with state-of-the-art  
70 recurrent network architectures (based on LSTM, GRU) on real-world machine learning  
71 benchmarks.
- 72 5. We show that EGRU exhibits high levels of activity-sparsity during both inference and  
73 learning.

## 74 2 Related work

75 Activity sparsity in RNNs has been proposed previously in various forms [28, 46, 47], but only  
76 focusing on achieving it during inference. Conditional computation is a form of activity sparsity  
77 used in [17] to scale to 1 trillion parameters. This architecture is based on the feedforward transformer  
78 architecture, with a separate network making the decision of which sub-networks should be active [59].  
79 An asynchronous event-based architecture was recently proposed specifically targeted towards graph  
80 neural networks [56]. QRNNs [7], SRUs[38] and IndrNNs [39] target increasing the parallelism in a  
81 recurrent network without directly using activity-sparsity. Unlike [17], our architecture uses a unit-local  
82 decision making process for the dynamic activity-sparsity, specifically for recurrent architecture. The  
83 cost of computation is lower in an EGRU compared to [47], and can be implemented to have parallel  
84 computation of intermediate updates between events, while also being activity sparse in its output.

85 Models based on sparse communication [64] for scalability have been proposed recently for  
86 feedforward networks, using locality sensitivity hashing to dynamically choose downstream  
87 units for communicating activations. This is a dynamic form of parameter-sparsity [25]. But,  
88 parameter/model-sparsity is, in general, orthogonal to and complementary with our method for  
89 activity-sparsity, and can easily be combined for additional gains.

90 Biologically realistic spiking networks [41] are often implemented using event-based updates and have  
 91 been scaled to huge sizes [33], albeit without any task-related performance evaluation. Models for  
 92 deep learning with recurrent spiking networks [3, 55] mostly focus on modeling biologically realistic  
 93 memory and learning mechanisms. Moreover, units in a spiking neural network implement dynamics  
 94 based on biology and communicate solely through unitary events, while units in an EGRU send  
 95 real-valued signals to other units, and have more general dynamics. A sparse learning rule was recently  
 96 proposed [4] that is a local approximation of backpropagation through time, but not event-based.

97 The event-based learning rule for the continuous time EGRU is inspired by, and a generalization of,  
 98 the event-prop learning rule for spiking neurons [63]. As in that paper, we use the adjoint method  
 99 for ordinary differential equations (ODEs) to train the continuous time EGRU [10, 50] combined with  
 100 sensitivity analysis for hybrid discrete/continuous systems [11, 19]. Using pseudo-derivatives for back-  
 101 propagating through the non-differential threshold function, as we use for our discrete-time EGRU, was  
 102 originally proposed for feedforward spiking networks in neuromorphic hardware in [16] and developed  
 103 further in [3, 65]. The sparsity of learning with BPTT when using appropriate pseudo-derivatives  
 104 in a discrete-time feed-forward spiking neural network was recently described in [49].

105 A continuous time version of sigmoidal RNNs was first proposed in [2] and for GRUs in [14]. The  
 106 latter used a Bayesian update for network states when input events were received, but the network itself  
 107 was not event-based. As in [37, 46], the focus there was on modeling irregularly spaced input data,  
 108 and not on event-based network simulation or activity-sparse inference and training. [9] also recently  
 109 proposed a continuous time recurrent network for more stable learning, without event-based mechanics.  
 110 GRUs were formulated in continuous time in [32], but purely for analyzing its autonomous dynamics.

### 111 3 Event-based GRU

#### 112 3.1 Time-sparse GRU formulation

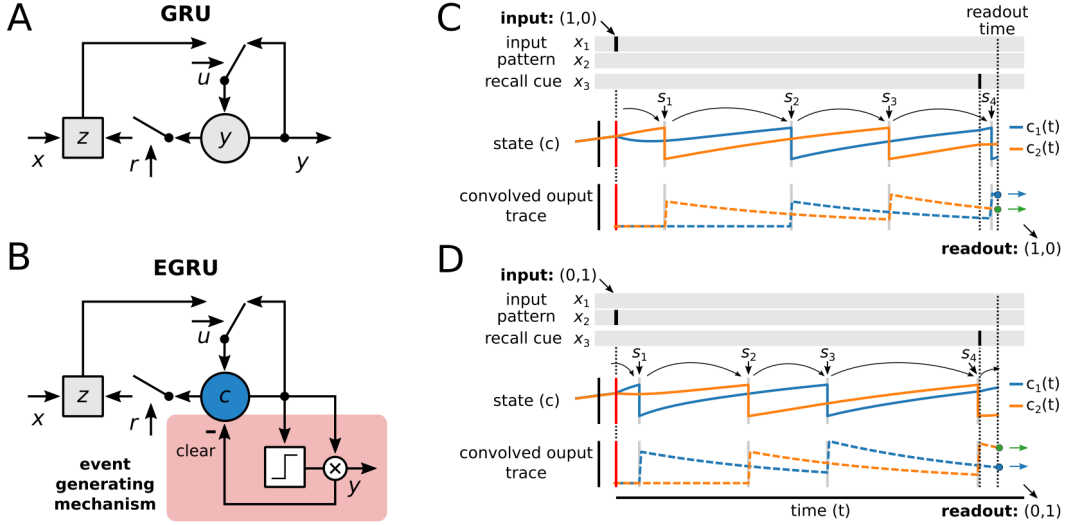


**Figure 1:** Illustration of EGRU. **A:** A single unit of the original GRU model adapted from [12]. **B:** EGRU unit with event generating mechanism. **C,D:** Dynamics of EGRU internal state variables for the delay-copy task with input  $(1,0)$  (C) and  $(0,1)$  (D). Colors are matched for neurons in both plots.

113 We base our model on the GRU [12], illustrated for convenience in Fig. 1A. It consists of internal  
 114 gating variables for updates ( $u$ ) and a reset ( $r$ ), that determine the behavior of the internal state  $y$ .  
 115 The state variable  $z$  determines the interaction between external input  $x$  and the internal state. The  
 116 dynamics of a layer of GRU units, at time step  $t$ , is given by the set of vector-valued update equations:

$$\begin{aligned} \mathbf{u}^{(t)} &= \sigma(\mathbf{W}_u [\mathbf{x}^{(t)}, \mathbf{y}^{(t-1)}] + \mathbf{b}_u), & \mathbf{r}^{(t)} &= \sigma(\mathbf{W}_r [\mathbf{x}^{(t)}, \mathbf{y}^{(t-1)}] + \mathbf{b}_r), \\ \mathbf{z}^{(t)} &= g(\mathbf{W}_z [\mathbf{x}^{(t)}, \mathbf{r}^{(t)} \odot \mathbf{y}^{(t-1)}] + \mathbf{b}_z), & \mathbf{y}^{(t)} &= \mathbf{u}^{(t)} \odot \mathbf{z}^{(t)} + (1 - \mathbf{u}^{(t)}) \odot \mathbf{y}^{(t-1)}, \end{aligned} \quad (1)$$

117 where  $\mathbf{W}_{u/r/z}$ ,  $\mathbf{b}_{u/r/z}$  denote network weights and biases,  $\odot$  denotes the element-wise (Hadamard)  
 118 product, and  $\sigma(\cdot)$  is the vectorized sigmoid function. The notation  $[\mathbf{x}^{(t)}, \mathbf{y}^{(t-1)}]$  denotes vector concate-  
 119 nation. The function  $g(\cdot)$  is an element-wise nonlinearity (typically the hyperbolic tangent function).

120 We introduce an event generating mechanisms by augmenting the GRU with a rectifier and a clearing  
 121 mechanism (see Fig. 1B for an illustration). This introduces an event-based variant of the internal  
 122 state variable  $y_i^{(t)}$ , that is nonzero when the internal dynamics reach a threshold  $\vartheta_i$  and is cleared  
 123 immediately afterwards. Formally, this can be included in the model by adding an auxiliary internal  
 124 state  $c_i^{(t)}$ , and replacing  $\mathbf{y}^{(t)} = (y_1^{(t)}, y_2^{(t)}, \dots)$  with the event-based form

$$y_i^{(t)} = c_i^{(t)} H(c_i^{(t)} - \vartheta_i) \quad \text{with} \quad c_i^{(t)} = u_i^{(t)} z_i^{(t)} + (1 - u_i^{(t)}) c_i^{(t-1)} - y_i^{(t-1)}, \quad (2)$$

125 where  $H(\cdot)$  is the Heaviside step function and  $\vartheta_i > 0$  is a trainable threshold parameter. This form  
 126 is well suited for time sparsity, since  $H(\cdot)$  acts here as a gating mechanism, by generating a single  
 127 non-zero output when  $c_i^{(t)}$  crosses the threshold  $\vartheta_i$ . That is, at all time steps  $t$  with  $c_i^{(t)} < \vartheta_i, \forall i$ , we  
 128 have  $y_i^{(t)} = 0$ . The  $-y_i^{(t-1)}$  term in Eq. (2) makes emission of multiple consecutive events by the same  
 129 unit unlikely, hence favoring overall sparse activity. With this formulation, each unit only needs to  
 130 be updated when an input is received either externally or from another unit in the network. This is  
 131 because, if both  $x_i^{(t)} = y_i^{(t-1)} = 0$  for the  $i$ -th unit, then  $u_i^{(t)}, r_i^{(t)}, z_i^{(t)}$  are essentially constants, and  
 132 hence the update for  $y_i^{(t)}$  can be retroactively calculated efficiently on the next incoming event.

### 133 3.2 Limit to continuous time

134 The discrete time model Eq. (1) considers the GRU dynamics only at integer time points,  
 135  $t_0 = 0, t_1 = 1, t_2 = 2, \dots$ . However, in general it is possible to express the GRU dynamics for an arbitrary  
 136 time step  $\Delta t$ , with  $t_n = t_{n-1} + \Delta t$ . The discrete time GRU dynamics can be intuitively interpreted  
 137 as an Euler discretization of an ordinary differential equation (ODE) [32] (see Supplement), which  
 138 we extend further to formulate the EGRU. This is equivalent to taking the continuous time limit  $\Delta t \rightarrow 0$   
 139 to get dynamics for the internal state  $\mathbf{c}(t)$  starting from the discrete time EGRU model outlined above.  
 140 In the resulting dynamical system equations inputs cause changes to the states only at the event times,  
 141 whereas the dynamics between events can be expressed through ODEs. To arrive at the continuous  
 142 time formulation we introduce the neuronal activations  $\mathbf{a}_u(t)$ ,  $\mathbf{a}_r(t)$  and  $\mathbf{a}_z(t)$ , with

$$\mathbf{u}(t) = \sigma(\mathbf{a}_u(t)), \quad \mathbf{r}(t) = \sigma(\mathbf{a}_r(t)), \quad \mathbf{z}(t) = g(\mathbf{a}_z(t)), \quad (3)$$

$$\text{with dynamics} \quad \tau_s \dot{\mathbf{a}}_X = -\mathbf{a}_X - \mathbf{b}_X, \quad X \in \{u, r, z\}$$

143 and

$$\tau_m \dot{\mathbf{c}}(t) = \mathbf{u}(t) \odot (\mathbf{z}(t) - \mathbf{c}(t)) = F(t, \mathbf{a}_u, \mathbf{a}_r, \mathbf{a}_z, \mathbf{c}), \quad (4)$$

144 where  $\tau_s$  and  $\tau_m$  are time constants,  $\mathbf{c}(t)$ ,  $\mathbf{u}(t)$  and  $\mathbf{z}(t)$  are the continuous time analogues to  $\mathbf{c}^{(t)}$ ,  
 145  $\mathbf{u}^{(t)}$  and  $\mathbf{z}^{(t)}$ , and  $\dot{\mathbf{a}}_X$  denotes the time derivative of  $\mathbf{a}_X$ . The boundary conditions are defined for  $t = 0$   
 146 as  $\mathbf{a}_X(0) = \mathbf{c}(0) = \mathbf{0}$ . The function  $F$  in Eq. (4) determines the behavior of the EGRU between event  
 147 times, i.e. when  $\mathbf{x}(t) = \mathbf{0}$  and  $\mathbf{y}(t) = \mathbf{0}$ . Nonzero external inputs and internal events cause jumps in  
 148  $\mathbf{c}(t)$  and  $\mathbf{a}_X(t)$ .

149 Furthermore, the formulation of the event generating mechanisms Eq.(2) introduced above can be  
 150 expressed in a straightforward manner in continuous time. Note that in continuous time the exact time  
 151  $s$  at which the internal variable  $c_i(s)$  reaches the threshold ( $c_i(s) = \vartheta_i$ ) can be determined with very  
 152 high precision. Therefore, the value of  $c_i(s)$  and the instantaneous amplitude of  $y_i(s)$  simultaneously  
 153 approach  $\vartheta_i$  at time point  $s$ , so that the  $-y_i$  term in Eq. (2) effectively resets  $c_i(s)$  to zero, right after  
 154 an event was triggered. To describe these dynamics we introduce the set of internal events  $\mathbf{e}$ ,  $e_k \in \mathbf{e}$ ,  
 155  $e_k = (s_k, n_k)$ , where  $s_k$  are the continuous (real-valued) event times, and  $n_k$  denotes which unit got  
 156 activated. An event  $e_k$  is triggered whenever  $c_{n_k}(t)$  reaches  $\vartheta$ . More precisely:

$$(s_k, n_k) : c_{n_k}^-(s_k) = \vartheta_{n_k}, \quad (5)$$

157 where the superscript  $\cdot^- (\cdot^+)$  denotes the quantity just before (after) the event. Immediately after  
 158 an event has been generated the internal state is cleared:  $c_{n_k}^+(s_k) = 0$ . At the time of this event, the

159 activations of all the units  $m \neq n_k$  connected to unit  $n_k$  experiences a jump in its state value. The jump  
 160 for  $a_{x,m}$  is given by:

$$a_{x,m}^+(s_k) = a_{x,m}^-(s_k) + w_{x,mn_k} r_{x,n_k} c_{n_k}^-(s_k), \quad (6)$$

161 where  $x \in \{u, r, z\}$ ,  $\mathbf{r}_x = 0$  when  $x \in \{u, z\}$  and  $\mathbf{r}_x = \mathbf{r}$  when  $x = \{r\}$ . This is equivalent to  $y_i = c_{n_k}^-$   
 162 being the output of each network unit. A similar jump is experienced on arrival of an external input,  
 163 using the appropriate input weights instead (see Supplement for specifics).

164 The continuous time event-based state update is illustrated in Fig. 1C and D for the delay-copy task  
 165 described in Section 4.1. Two EGRU units are used here and states  $c_i(t)$  and event times  $s_k$  are shown.  
 166 At the beginning of the trial an input pattern ( $x_1 = 1$ ,  $x_2 = 0$ , and  $x_1 = 0$ ,  $x_2 = 1$  in Fig. 1C and D,  
 167 respectively) has to be memorized in the network and retrieved again after the recall cue ( $x_3 = 1$ )  
 168 was given. The parameters are trained with the event-based updates described in Section 3.3. The  
 169 required memory is stored in the internal events and state dynamics. State updates can be performed  
 170 in an event-based fashion, i.e. by jumping from one event time  $s_k$  to the next  $s_{k+1}$ . In-between state  
 171 values follow the state dynamics Eq.(4) and their values are not needed to perform the updates (but  
 172 are shown here for the sake of illustration). By construction, the state updates for external and internal  
 173 events only happen on receipt of event. Since Eqs. (3), (4) are linear ODEs, the intermediate updates  
 174 due to autonomous state dynamics can also be performed cumulatively and efficiently just at event  
 175 times, hence avoiding any computation in the absence of incoming events.

### 176 3.3 Event-based gradient-descent using adjoint method

177 To derive the event-based gradient updates for the EGRU we define the loss over duration  $T$  as  
 178  $\int_0^T \ell_c(\mathbf{c}(t), t) dt$ , where  $\ell_c(\mathbf{c}(t), t)$  is the instantaneous loss at time  $t$ .  $T$  is a task-specific time duration  
 179 within which the training samples are given to the network as events, and the outputs are read out. In  
 180 general  $\ell_c(\mathbf{c}(t), t)$  may depend arbitrarily on  $\mathbf{c}(t)$ , however in practice we choose the instantaneous loss  
 181 to depend on the EGRU states only at specific output times to adhere to our fully event-based algorithm.

182 The loss is augmented with the terms containing the Lagrange multipliers  $\lambda_c, \lambda_{a_x}$  to add constraints  
 183 defining the dynamics of the system from Eqs. (3), (4). The total loss  $\mathcal{L}$  thus reads

$$\mathcal{L} = \int_0^T \left[ \ell_c(\mathbf{c}(t), t) + \lambda_c \cdot (\tau_m \dot{\mathbf{c}}(t) - F(t, \mathbf{a}_u, \mathbf{a}_r, \mathbf{a}_z, \mathbf{c})) + \sum_{x \in \{u, r, z\}} \lambda_{a_x} \cdot (\tau_s \dot{\mathbf{a}}_x + \mathbf{a}_x) \right] dt. \quad (7)$$

184 The Lagrange multipliers are referred to as the adjoint variables in this context, and may be chosen  
 185 freely since both  $\tau_m \dot{\mathbf{c}}(t) - F(t, \mathbf{a}_u, \mathbf{a}_r, \mathbf{a}_z, \mathbf{c})$  and  $\tau_s \dot{\mathbf{a}}_x + \mathbf{a}_x$  are everywhere zero by construction.

186 We can choose dynamics and jumps at events for the adjoint variables in such a way that they can  
 187 be used to calculate the gradient  $\frac{d\mathcal{L}}{dw_{ji}}$ . Calculating the partial derivatives taking into account the  
 188 discontinuous jumps at event times depends on the local application of the implicit function theorem,  
 189 which requires event times to be a differentiable function of the parameters. See [10, 19, 63] for a  
 190 description of applying the adjoint method for hybrid discrete/continuous time systems with further  
 191 theoretical background, and the Supplement for a derivation specific to the EGRU.

192 The time dynamics of the adjoint variables is given by the following equations with a boundary  
 193 condition of  $\lambda_c(T) = \lambda_{a_x}(T) = 0$ :

$$\left( \frac{\partial F}{\partial \mathbf{c}} \right)^T \lambda_c - \tau_m \dot{\lambda}_c = 0, \quad \lambda_{a_x} + \left( \frac{\partial F}{\partial \mathbf{a}_x} \right)^T \lambda_c - \tau_s \dot{\lambda}_{a_x} = 0, \quad (8)$$

194 for  $x \in \{u, r, z\}$ , and  $M^T$  denoting the transpose of the matrix  $M$ . The event updates for the adjoints  
 195 are described in the Supplement. In practice, the integration of  $\lambda$  is done backwards in time.

196 For the recurrent weights  $w_{x,ij}$  from the different parameter matrices  $W_x$  for  $x \in u, r, z$ , we can write  
 197 the weight updates using only quantities calculated at events  $e_k$  as:

$$\Delta w_{x,ij} = \frac{\partial}{\partial w_{x,ij}} \mathcal{L}(\mathbf{W}) = \sum_k \xi_{x,ijk}. \quad (9)$$

198 The corresponding value of  $\xi_{x,ijk} = (\xi_{x,k})_{ij}$  is given by the following formula, written in vector form  
 199 for succinctness:

$$\xi_{x,k} = -\tau_s (\mathbf{r}_x^-(s_k) \odot \mathbf{c}^-(s_k)) \otimes \lambda_{a_x}^+(s_k), \quad (10)$$

200 where  $\otimes$  is the outer product,  $c^-$  refers to the value of  $c(t)$  just before event  $e_k$ ,  $\mathbf{r}_x^- = 0$  for  $x \in \{u, z\}$   
 201 and equal to the value of  $\mathbf{r}(t)$  just before event  $e_k$  for  $x = \{r\}$ ,  $\lambda_{\alpha_x}^+$  refers to the value of the adjoint  
 202 variable  $\lambda_{\alpha_x}(t)$  just after the event  $e_k$ . Thus, the values of  $\mathbf{r}(t), c(t)$  needs to be stored only at event  
 203 times, and  $\lambda_{\alpha_x}(t)$  needs to be calculated only at these times, making the gradient updates event-based.  
 204 See the Supplement for the update rules for the input weights and biases.

### 205 3.4 Sparse approximate BPTT in discrete time

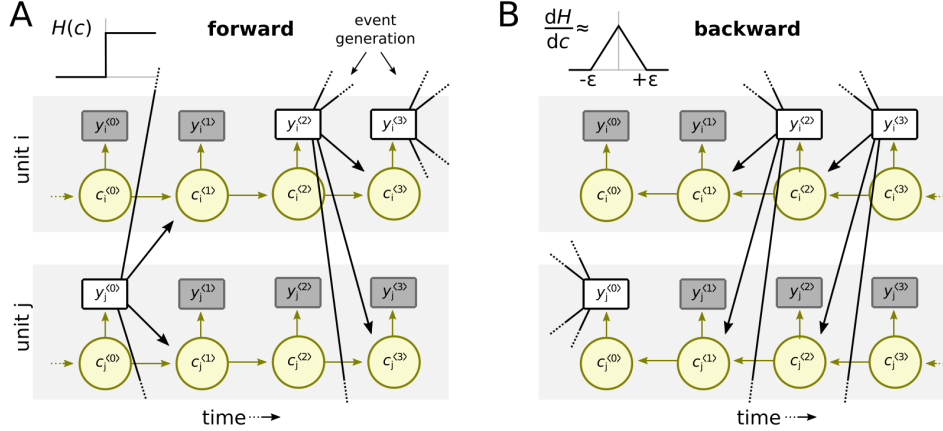


**Figure 2:** Illustrate the discrete time state dynamics for two EGRU units ( $i$  and  $j$ ). **A:** Forward dynamics. Information only propagates from units that generate an event. **B:** Activity-sparse backward dynamics. Insets show threshold function  $H(c)$  and pseudo derivative thereof.

206 In discrete time, the network uses a threshold activation function  $H(c)$  to decide whether to emit an event  
 207 as described in Eq. (2). Since  $H(c)$  is not differentiable at the threshold  $\vartheta_i$ , we define a pseudo-derivative  
 208 at that point for calculating the backpropagated gradients. The pseudo-derivative is defined as a piece-  
 209 wise linear function that is non-zero for values of state  $c_i$  between  $\vartheta_i + \epsilon$  and  $\vartheta_i - \epsilon$  as shown in the inset  
 210 in Fig. 2B. Since the pseudo-derivative is zero whenever the internal state of the unit is below  $\vartheta_i - \epsilon$ , the  
 211 backpropagated gradients are also 0 for all such units, making the backward-pass sparse (see Fig.2 for  
 212 an illustration). Note that the case where the internal unit state is above  $\vartheta_i + \epsilon$  tends to occur less often,  
 213 since the unit will emit an event and the internal state will be cleared (Eq. (2)) at the next simulation step.

### 214 3.5 Computation and memory reduction due to sparsity

215 For the forward pass of the discrete time EGRU, an activity sparsity of  $\alpha$  (i.e. an average of  $\alpha$  events  
 216 per simulation step) leads to the reduction of multiply-accumulate operations (MAC), by factor  $\alpha$ .  
 217 We focus on MAC operations, since they are by far the most expensive compute operation in these  
 218 models. If optimally implemented an activity sparsity of 80% will require 80% fewer MAC operations  
 219 compared to a GRU that is not activity-sparse. Computation related to external input is only performed  
 220 at input times, and hence is as sparse as the input, both in time and space. During the backward pass, a  
 221 similar factor of computational reduction is observed, based on the backward-pass sparsity  $\beta$  which is,  
 222 in general, less than  $\alpha$ . This is because, when the internal state value is not within  $\pm\epsilon$  of the threshold  
 223  $\vartheta$ , the backward pass is skipped, as described in section 3.4. Since our backward pass is also sparse, we  
 224 expect to need to store only  $\beta$  fraction of the activations for later use, hence also reducing the memory  
 225 usage. In all our experiments, we report activity-sparsity values calculated through simulations.

## 226 4 Results

### 227 4.1 Delay-copy task

228 To illustrate the behavior of the continuous-time EGRU model (Fig. 1C,D) we used a simple delay-copy  
 229 task (also called the copy memory task [24]). A binary vector was presented to the network at the input  
 230 time. This was followed by a delay period, after which the network was given a cue input indicating  
 231 that it should recall the input seen before. A small network with only two EGRU units was used here,  
 232 trained with the event-based learning rules described in Section 3.3. Right after the cue input, the  
 233 network had to report the memorized input pattern. EGRU outputs  $y_i$  emitted at network event times  
 234 were convolved with an exponential kernel to retrieve output traces, which were then used to retrieve

235 the stored binary patterns based on their relative magnitudes. The kernel time constant was chosen  
 236 to be significantly lower than the delay time such that the network had to retain the memory in the event  
 237 dynamics. The binary cross-entropy loss was used to train this model until it reached perfect (100%)  
 238 bitwise accuracy on this task. Fig. 1C,D shows the dynamics of the continuous-time model after  
 239 training, as well as the output trace and events. The network has learned to generate events such that  
 240 output traces reliably encode the stored input patterns. [Supplemental Table S1 shows the robustness](#)  
 241 [of the training for different sizes of inputs, networks, delay periods, all for multiple runs.](#)

## 242 4.2 Gesture prediction

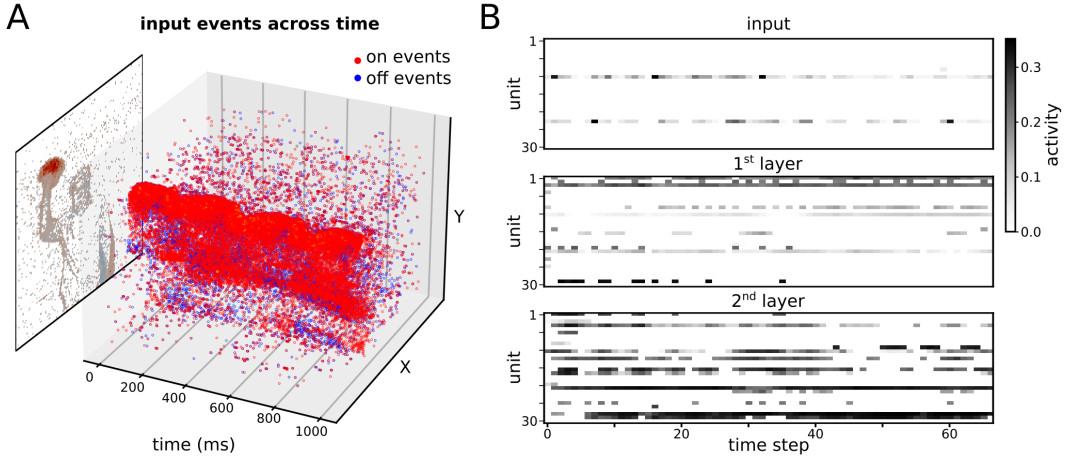


**Figure 3:** **A:** Illustration of DVS gesture classification data for an example class (right hand wave). On (red) and off (blue) events are shown over time and merged into a summary image for illustration (not presented to the network). **B:** Sparse activity of input and EGRU units (random subset of 30 units shown for each layer).

243 We next evaluate our model on gesture prediction, which is a popular real-world benchmark for RNNs.  
 244 Here and in the remainder of the experiments we used the discrete time version of EGRU, since it is  
 245 easier to implement and use while retaining most of the advantages of the continuous time model. We  
 246 use the DVS128 Gesture Dataset [1], where the inputs are defined as events. This dataset is widely used  
 247 in neuromorphic research and enables us to demonstrate our model’s performance and computational  
 248 efficiency on event-based data. The dataset contains 11 gestures from 29 subjects recorded with a  
 249 DVS128 event camera [40]. Each event encodes a relative change of illumination and is given as  
 250 spatio-temporal coordinates of X/Y position on the  $128 \times 128$ -pixel sensor and time stamp. Raw event  
 251 times were combined into ‘frames’ by binning them over time windows of 25 ms. Frames were then  
 downsampled to  $32 \times 32$  pixels using a maxpool layer.

reference	architecture (# units)	para- meters	effective MAC	accu- racy	activity sparsity	backward sparsity
He et al. [23]	LSTM (512)	7.35M	7.34M	86.81%	-	-
Innocenti et al. [30]	AlexNet+LSTM+DA	9.99M	638.25M	97.73%	-	-
<b>ours</b>	GRU (1024)	15.75M	15.73M	88.07%	0%	-
<b>ours</b>	<b>EGRU</b> (512)	5.51M	4.19M	88.02%	83.79%	53.55%
<b>ours</b>	<b>EGRU</b> (1024)	15.75M	10.54M	90.22%	82.53%	56.63%
<b>ours</b>	<b>EGRU+DA</b> (1024)	15.75M	10.77M	97.13%	78.77%	58.20%

**Table 1:** Model comparison for the DVS Gesture recognition task. Effective number of MAC operations as described in section 3.5.

252

253 Unlike previous approaches that focused on a feedforward/RNN hybrid approach [1, 20, 30], we focused  
 254 on pure RNN based architectures following the work of [23]. A binary cross-entropy loss was applied  
 255 with an additional regularization loss on the output gate to produce 5% activity and the state variable  $c$  to  
 256 be slightly below the threshold. The models were trained using the Adam optimizer for 1000 epochs to



257 verify their stability but typically reached a plateau performance after 200 epochs (see Supplement for  
 258 further details). Due to this, backward sparsity as described in Section 3.5 was calculated at epoch 100.

259 Comparison of model performance on gesture prediction is presented in Table 1. The model had  
 260 inherent activity-sparsity of 70% which the regularization increased to 90% without significant  
 261 performance decrease. EGRU consistently outperformed GRU networks of the same size on this task  
 262 by a small margin. Adding data augmentation (DA) by applying random crop, translation, and rotation,  
 263 as previously done in [30], increased the performance to over 97% of this pure RNN architecture,  
 264 coming close to state-of-the-art architectures that even include costly AlexNet pre-processing. [Further  
 265 experimental details, ablation studies and statistics over different runs can be found in the supplement  
 266 sections D.1, D.1.1 and tables S3, S4 respectively.](#)

### 267 4.3 Sequential MNIST

268 Next, we tested the EGRU on the sequential MNIST task [36], which is a widely used benchmark  
 269 for recurrent networks. In this task, the MNIST handwritten digits were given as input one pixel at a  
 270 time, and at the end of the input sequence, the network output was used to classify the digit. We trained  
 271 a 1-layer EGRU with 590 units (matching the number of parameters with a 512 unit LSTM). We did  
 272 not use any regularisation to increase sparsity in this task, so that we could test how much sparsity, both  
 273 forward and backward, arises naturally in the EGRU. In Table 2, we report the results of discrete-time  
 274 EGRU along with other state-of-the-art architectures. EGRU achieved a task performance comparable  
 275 to previous architectures while using much fewer operations (more than an 5-fold reduction in effective  
 276 MAC operations compared to GRU). [Further experimental details, and statistics over different runs  
 277 can be found in the supplement sections D.2 and table S5 respectively.](#)

reference	architecture (# units)	parameters	effective MAC	test accuracy	activity sparsity
Rusch and Mishra [54]	coRNN (256)	134K	262K	99.4%	-
Gu et al. [22]	LSTM (512)	1M	1M	98.8%	-
<b>ours</b>	GRU (590)	1M	1M	98.8%	-
<b>ours</b>	<b>EGRU (590)</b>	1M	226K	98.3%	72.1%

**Table 2:** Model comparison on sequential MNIST task. Top-1 test scores, given as percentage accuracy, where higher is better.

### 278 4.4 Language Modeling

279 Natural language processing is a popular domain for benchmarking recurrent neural networks. We  
 280 evaluated our model on a language modeling task based on the PennTreebank [42] dataset to validate  
 281 the functionality of our model. While techniques such as neural cache models [21] or dynamic  
 282 evaluation [35] have been shown to improve language models, we focused on the RNN model itself in  
 283 this work, taking [45] as our baseline. Following [45], our models consists of a dense 400-dimensional  
 284 embedding layer, and three stacked RNN cells with DropConnect applied to the hidden-to-hidden  
 285 weights [61]. The weights of the final softmax layer were tied to the embedding layer [29, 51]. All  
 286 our models are optimized with Adam for 1000 epochs, and parameters were tuned for each model  
 287 individually. Details on training and model parameters can be found in the Supplement. Results are  
 288 shown in Table 3. In our experiments, GRUs did not reach the performance of LSTM variants on  
 289 this task, which, to the best of our knowledge, is consistent with recent RNN language modeling  
 290 literature [44, 45]. At the same time, EGRU slightly outperformed GRU, while maintaining high levels  
 291 of activity sparsity. [Further experimental details, and statistics over different runs can be found in  
 292 the supplement sections D.3 and table S6 respectively.](#)

## 293 5 Discussion

294 We have introduced EGRU, a new form of a recurrent neural network that is competitive with current  
 295 deep recurrent models yet can efficiently perform both inference and learning. To achieve this, we  
 296 first formulated the GRU in continuous time and converted it to an event-based form that achieved  
 297 activity-sparsity naturally. Furthermore, the gradient-descent updates on this time-continuous EGRU  
 298 mirrored the activity sparsity of the inference. We then demonstrated a discrete-time simplification  
 299 of this model that also exhibited event-based activity-sparse inference and learning while being easier  
 300 to implement with popular ML frameworks such as PyTorch or Tensorflow.



reference	architecture (# units)	para- meters	effective MAC *	validation	test	activity sparsity
Gal et al. [18]	Variational LSTM	24M	-	77.3	75.0	-
Melis et al. [44]	1 layer LSTM	24M	-	61.8	59.6	-
Merity et al. [45]	AWD-LSTM	24M	24M	60.0	57.3	-
<b>ours</b>	GRU (1350)	24M	24M	71.2	68.8	-
<b>ours</b>	<b>EGRU</b> (1350)	24M	4.7M	67.4	64.5	88.0%
<b>ours</b>	<b>EGRU</b> (2000)	45M	6.6M	66.5	63.7	90.4%
<b>ours</b>	<b>EGRU</b> (2700)	77M	8.1M	66.4	63.5	93.2%

**Table 3:** Model comparison on PennTreebank. Validation and test scores are given as perplexities, where lower is better. Sparsity refers to activity-sparsity of the EGRU output, and effective MAC operations consider the layer-wise sparsity in the forward pass. \*

301 The EGRU achieved competitive task performance on various real-world tasks such as gesture  
302 recognition and language modeling while achieving a sparsity of up to 80% for the gesture recognition  
303 task and 90% on the language modeling task. Scaling up networks for language modeling has shown  
304 some of the most promising results in the last few years [8, 17] Hence our choice of task, albeit on  
305 a smaller scale, was to validate the functionality of the model. Considering the need for extensive  
306 hyperparameter search [44] for language modeling, our model achieved promising results while  
307 maintaining a high degree of activity-sparsity. For example, our EGRU with 1350 hidden units reached  
308 perplexities comparable with LSTM and GRU, while maintaining an activity-sparsity of 86 % (14%  
309 of the units active on average). The amount of computation used by an EGRU also scales sub-linearly  
310 with an increase in the size of the network and number of parameters, making it a scalable alternative  
311 to LSTM/GRU based architectures (see Supplement).

312 While we use the GRU as the basis for our model due to its simplicity, this formulation can easily be ex-  
313 tended to any arbitrary network dynamics, including the LSTM, allowing specialized architectures for  
314 different domains. The adjoint method for hybrid systems that we use here is a powerful general-purpose  
315 tool for training event-based activity-sparse forms of various recurrent neural network architectures.  
316 Another novel outcome of this paper is that this theory can handle inputs in continuous time as events,  
317 which is very intuitive, hence providing an alternative to the more complex controlled differential  
318 equations [34]. The EGRU can also be used for irregularly spaced sequential data quite naturally.

319 The compute efficiency of this model can directly translate into gains in energy efficiency when  
320 implemented using event-based software primitives. These same properties would also allow the  
321 model to work well on heterogenous compute resources, including pure CPU nodes, and neuromorphic  
322 devices such as Intel’s Loihi [13] and SpiNNaker 2 [27], that can achieve orders of magnitude higher  
323 energy efficiency. The EGRU model will also perform well in more mainstream deep learning  
324 hardware that is enabled for dynamic sparsity, such as the Graphcore system [31]. On neuromorphic  
325 devices with on-chip memory in the form of a crossbar array, the activity sparsity directly translates  
326 into energy efficiency. For larger models that need off-chip memory, activity-sparsity needs to be  
327 combined with parameter-sparsity to reduce energy-intensive memory access operations.

328 In summary, starting with the motivation of building scalable, energy-efficient deep recurrent models,  
329 we demonstrated the EGRU, which reduces the required compute for both inference and learning by  
330 enhancing sparsity in the network. This approach lays the foundation for exploring novel capabilities  
331 that can emerge from scaling up RNNs similar to what has been seen for feed-forward architectures  
332 in recent years.

333 **Potential negative societal impact:** The proposed model is a new variant of the previously published  
334 GRU and would therefore essentially inherit all potential negative societal impacts from that model,  
335 including the potential risks that come with automated surveillance systems, vulnerability to fraud and  
336 adversarial attacks, etc. (see [6] and [62] for critical reviews). However, the model also provides the  
337 potential societal benefit of making these models more energy-efficient and thus reducing the energy  
338 and carbon footprint of machine learning. Scaling this model to larger sizes, especially for language  
339 modeling, can lead to the same problems as current large language models [5]. The effect of activity  
340 sparsity on prediction bias needs to be studied further in the same way as for parameter sparsity [26].

## References

- 341
- 342 [1] A. Amir, B. Taba, D. Berg, T. Melano, J. McKinstry, C. Di Nolfo, T. Nayak, A. Andreopoulos,  
343 G. Garreau, M. Mendoza, et al. A low power, fully event-based gesture recognition system.  
344 In *Proceedings of the IEEE conference on computer vision and pattern recognition*, pages  
345 7243–7252, 2017.
- 346 [2] R. D. Beer. On the Dynamics of Small Continuous-Time Recurrent Neural Networks. *Adaptive*  
347 *Behavior*, 3(4):469–509, Mar. 1995. ISSN 1059-7123. doi: 10.1177/105971239500300405.
- 348 [3] G. Bellec, D. Salaj, A. Subramoney, R. Legenstein, and W. Maass. Long short-term memory  
349 and Learning-to-learn in networks of spiking neurons. In S. Bengio, H. Wallach, H. Larochelle,  
350 K. Grauman, N. Cesa-Bianchi, and R. Garnett, editors, *Advances in Neural Information*  
351 *Processing Systems 31*, pages 787–797. Curran Associates, Inc., 2018.
- 352 [4] G. Bellec, F. Scherr, A. Subramoney, E. Hajek, D. Salaj, R. Legenstein, and W. Maass. A solution  
353 to the learning dilemma for recurrent networks of spiking neurons. *Nature Communications*,  
354 11(1):3625, July 2020. ISSN 2041-1723. doi: 10.1038/s41467-020-17236-y.
- 355 [5] E. M. Bender, T. Gebru, A. McMillan-Major, and S. Shmitchell. On the dangers of stochastic  
356 parrots: Can language models be too big? In *Proceedings of the 2021 ACM Conference on*  
357 *Fairness, Accountability, and Transparency*, pages 610–623, 2021.
- 358 [6] A. Birhane, P. Kalluri, D. Card, W. Agnew, R. Dotan, and M. Bao. The values encoded in  
359 machine learning research. *arXiv preprint arXiv:2106.15590*, 2021.
- 360 [7] J. Bradbury, S. Merity, C. Xiong, and R. Socher. Quasi-Recurrent Neural Networks.  
361 *arXiv:1611.01576 [cs]*, Nov. 2016.
- 362 [8] T. B. Brown, B. Mann, N. Ryder, M. Subbiah, J. Kaplan, P. Dhariwal, A. Neelakantan, P. Shyam,  
363 G. Sastry, A. Askell, S. Agarwal, A. Herbert-Voss, G. Krueger, T. Henighan, R. Child, A. Ramesh,  
364 D. M. Ziegler, J. Wu, C. Winter, C. Hesse, M. Chen, E. Sigler, M. Litwin, S. Gray, B. Chess,  
365 J. Clark, C. Berner, S. McCandlish, A. Radford, I. Sutskever, and D. Amodei. Language Models  
366 are Few-Shot Learners. *arXiv:2005.14165 [cs]*, July 2020.
- 367 [9] B. Chang, M. Chen, E. Haber, and E. H. Chi. AntisymmetricRNN: A Dynamical System View  
368 on Recurrent Neural Networks. *arXiv:1902.09689 [cs, stat]*, Feb. 2019.
- 369 [10] R. T. Q. Chen, Y. Rubanova, J. Bettencourt, and D. K. Duvenaud. Neural Ordinary Differential  
370 Equations. In S. Bengio, H. Wallach, H. Larochelle, K. Grauman, N. Cesa-Bianchi, and  
371 R. Garnett, editors, *Advances in Neural Information Processing Systems 31*, pages 6572–6583.  
372 Curran Associates, Inc., 2018.
- 373 [11] R. T. Q. Chen, B. Amos, and M. Nickel. Learning Neural Event Functions for Ordinary  
374 Differential Equations. In *International Conference on Learning Representations*, Sept. 2020.  
375 URL [https://openreview.net/forum?id=kW\\_zpEmMLdP](https://openreview.net/forum?id=kW_zpEmMLdP).
- 376 [12] K. Cho, B. Van Merriënboer, C. Gulcehre, D. Bahdanau, F. Bougares, H. Schwenk, and Y. Bengio.  
377 Learning phrase representations using rnn encoder-decoder for statistical machine translation.  
378 *arXiv preprint arXiv:1406.1078*, 2014.
- 379 [13] M. Davies, N. Srinivasa, T.-H. Lin, G. China, Y. Cao, S. H. Choday, G. Dimou, P. Joshi,  
380 N. Imam, S. Jain, et al. Loihi: A neuromorphic manycore processor with on-chip learning. *Ieee*  
381 *Micro*, 38(1):82–99, 2018.
- 382 [14] E. De Brouwer, J. Simm, A. Arany, and Y. Moreau. GRU-ODE-Bayes: Continuous Modeling  
383 of Sporadically-Observed Time Series. In *Advances in Neural Information Processing Systems*,  
384 volume 32. Curran Associates, Inc., 2019. URL [https://proceedings.neurips.cc/  
385 paper/2019/hash/455cb2657aaa59e32fad80cb0b65b9dc-Abstract.html](https://proceedings.neurips.cc/paper/2019/hash/455cb2657aaa59e32fad80cb0b65b9dc-Abstract.html).
- 386 [15] M. Dehghani, S. Gouws, O. Vinyals, J. Uszkoreit, and L. Kaiser. Universal Transformers.  
387 In *International Conference on Learning Representations*, Sept. 2018. URL [https://  
388 openreview.net/forum?id=HyzdRiR9Y7&noteId=HyxfZDmCk4&noteId=rkginvfklN](https://openreview.net/forum?id=HyzdRiR9Y7&noteId=HyxfZDmCk4&noteId=rkginvfklN).

- 389 [16] S. K. Esser, P. A. Merolla, J. V. Arthur, A. S. Cassidy, R. Appuswamy, A. Andreopoulos,  
390 D. J. Berg, J. L. McKinstry, T. Melano, D. R. Barch, C. di Nolfo, P. Datta, A. Amir,  
391 B. Taba, M. D. Flickner, and D. S. Modha. Convolutional networks for fast, energy-efficient  
392 neuromorphic computing. *Proceedings of the National Academy of Sciences*, 113(41):  
393 11441–11446, Nov. 2016. ISSN 0027-8424, 1091-6490. doi: 10.1073/pnas.1604850113. URL  
394 <http://www.pnas.org/content/113/41/11441>.
- 395 [17] W. Fedus, B. Zoph, and N. Shazeer. Switch Transformers: Scaling to Trillion Parameter Models  
396 with Simple and Efficient Sparsity. *arXiv:2101.03961 [cs]*, Jan. 2021.
- 397 [18] Y. Gal and Z. Ghahramani. A theoretically grounded application of dropout in recur-  
398 rent neural networks. In D. Lee, M. Sugiyama, U. Luxburg, I. Guyon, and R. Garnett,  
399 editors, *Advances in Neural Information Processing Systems*, volume 29. Curran As-  
400 sociates, Inc., 2016. URL [https://proceedings.neurips.cc/paper/2016/file/  
401 076a0c97d09cf1a0ec3e19c7f2529f2b-Paper.pdf](https://proceedings.neurips.cc/paper/2016/file/076a0c97d09cf1a0ec3e19c7f2529f2b-Paper.pdf).
- 402 [19] S. Galán, W. F. Feehery, and P. I. Barton. Parametric sensitivity functions for hybrid  
403 discrete/continuous systems. *Applied Numerical Mathematics*, 31(1):17–47, Sept. 1999. ISSN  
404 0168-9274. doi: 10.1016/S0168-9274(98)00125-1.
- 405 [20] R. Ghosh, A. Gupta, A. Nakagawa, A. Soares, and N. Thakor. Spatiotemporal filtering for  
406 event-based action recognition, 2019. URL <https://arxiv.org/abs/1903.07067>.
- 407 [21] E. Grave, A. Joulin, and N. Usunier. Improving neural language models with a continuous  
408 cache. In *5th International Conference on Learning Representations, ICLR 2017, Toulon,  
409 France, April 24-26, 2017, Conference Track Proceedings*. OpenReview.net, 2017. URL  
410 <https://openreview.net/forum?id=B184E5qee>.
- 411 [22] A. Gu, C. Gulcehre, T. Paine, M. Hoffman, and R. Pascanu. Improving the Gating  
412 Mechanism of Recurrent Neural Networks. In *Proceedings of the 37th Interna-  
413 tional Conference on Machine Learning*, pages 3800–3809. PMLR, Nov. 2020. URL  
414 <https://proceedings.mlr.press/v119/gu20a.html>.
- 415 [23] W. He, Y. Wu, L. Deng, G. Li, H. Wang, Y. Tian, W. Ding, W. Wang, and Y. Xie. Comparing  
416 snns and rnns on neuromorphic vision datasets: Similarities and differences. *Neural Networks*,  
417 132:108–120, 2020.
- 418 [24] S. Hochreiter and J. Schmidhuber. Long Short-Term Memory. *Neural Computation*, 9(8):  
419 1735–1780, Nov. 1997. ISSN 0899-7667. doi: 10.1162/neco.1997.9.8.1735.
- 420 [25] T. Hoefler, D. Alistarh, T. Ben-Nun, N. Dryden, and A. Peste. Sparsity in deep learning: Pruning  
421 and growth for efficient inference and training in neural networks. *Journal of Machine Learning  
422 Research*, 22(241):1–124, 2021.
- 423 [26] S. Hooker, A. Courville, G. Clark, Y. Dauphin, and A. Frome. What do compressed deep neural  
424 networks forget? *arXiv preprint arXiv:1911.05248*, 2019.
- 425 [27] S. Höppner, Y. Yan, B. Vogginger, A. Dixius, J. Partzsch, F. Neumärker, S. Hartmann, S. Schiefer,  
426 S. Scholze, G. Ellguth, et al. Dynamic voltage and frequency scaling for neuromorphic many-core  
427 systems. In *2017 IEEE International Symposium on Circuits and Systems (ISCAS)*, pages 1–4.  
428 IEEE, 2017.
- 429 [28] K. L. Hunter, L. Spracklen, and S. Ahmad. Two sparsities are better than one: Unlocking the  
430 performance benefits of sparse-sparse networks, 2021.
- 431 [29] H. Inan, K. Khosravi, and R. Socher. Tying word vectors and word classifiers: A loss framework  
432 for language modeling. In *5th International Conference on Learning Representations, ICLR  
433 2017, Toulon, France, April 24-26, 2017, Conference Track Proceedings*. OpenReview.net, 2017.  
434 URL <https://openreview.net/forum?id=r1aPbsFle>.
- 435 [30] S. U. Innocenti, F. Becattini, F. Pernici, and A. Del Bimbo. Temporal binary representation for  
436 event-based action recognition. In *2020 25th International Conference on Pattern Recognition  
437 (ICPR)*, pages 10426–10432. IEEE, 2021.

- 438 [31] Z. Jia, B. Tillman, M. Maggioni, and D. P. Scarpazza. Dissecting the graphcore ipu architecture  
439 via microbenchmarking. *arXiv preprint arXiv:1912.03413*, 2019.
- 440 [32] I. D. Jordan, P. A. Sokół, and I. M. Park. Gated recurrent units viewed through the lens of  
441 continuous time dynamical systems. *Frontiers in computational neuroscience*, page 67, 2021.
- 442 [33] J. Jordan, T. Ippen, M. Helias, I. Kitayama, M. Sato, J. Igarashi, M. Diesmann, and S. Kunkel.  
443 Extremely Scalable Spiking Neuronal Network Simulation Code: From Laptops to Exascale  
444 Computers. *Frontiers in Neuroinformatics*, 12:2, 2018. ISSN 1662-5196.
- 445 [34] P. Kidger, J. Morrill, J. Foster, and T. Lyons. Neural controlled differential equations for irregular  
446 time series. *Advances in Neural Information Processing Systems*, 33:6696–6707, 2020.
- 447 [35] B. Krause, E. Kahembwe, I. Murray, and S. Renals. Dynamic evaluation of neural sequence  
448 models. In J. Dy and A. Krause, editors, *Proceedings of the 35th International Conference on*  
449 *Machine Learning*, volume 80 of *Proceedings of Machine Learning Research*, pages 2766–2775.  
450 PMLR, 10–15 Jul 2018. URL <https://proceedings.mlr.press/v80/krause18a.html>.
- 451 [36] Q. V. Le, N. Jaitly, and G. E. Hinton. A simple way to initialize recurrent networks of rectified  
452 linear units. *arXiv preprint arXiv:1504.00941*, 2015.
- 453 [37] M. Lechner and R. Hasani. Learning Long-Term Dependencies in Irregularly-Sampled Time  
454 Series. *arXiv:2006.04418 [cs, stat]*, Dec. 2020. URL <http://arxiv.org/abs/2006.04418>.
- 455 [38] T. Lei, Y. Zhang, S. I. Wang, H. Dai, and Y. Artzi. Simple Recurrent Units for Highly  
456 Parallelizable Recurrence. *arXiv:1709.02755 [cs]*, Sept. 2017.
- 457 [39] S. Li, W. Li, C. Cook, C. Zhu, and Y. Gao. Independently Recurrent Neural Network (IndRNN):  
458 Building A Longer and Deeper RNN. *arXiv:1803.04831 [cs]*, May 2018.
- 459 [40] P. Lichtsteiner, C. Posch, and T. Delbruck. A  $128 \times 128$  120 dB  $15 \mu\text{s}$  latency asynchronous  
460 temporal contrast vision sensor. *IEEE journal of solid-state circuits*, 43(2):566–576, 2008.
- 461 [41] W. Maass. Networks of spiking neurons: the third generation of neural network models. *Neural*  
462 *networks*, 10(9):1659–1671, 1997.
- 463 [42] M. P. Marcus, M. A. Marcinkiewicz, and B. Santorini. Building a large annotated corpus of  
464 english: The penn treebank. *Comput. Linguist.*, 19(2):313–330, jun 1993. ISSN 0891-2017.
- 465 [43] C. Mead. How we created neuromorphic engineering. *Nature Electronics*, 3(7):434–435, 2020.
- 466 [44] G. Melis, C. Dyer, and P. Blunsom. On the state of the art of evaluation in neural language  
467 models. In *6th International Conference on Learning Representations, ICLR 2018, Vancouver,*  
468 *BC, Canada, April 30 - May 3, 2018, Conference Track Proceedings*. OpenReview.net, 2018.  
469 URL <https://openreview.net/forum?id=ByJHuTgA->.
- 470 [45] S. Merity, N. S. Keskar, and R. Socher. Regularizing and Optimizing LSTM Language Models.  
471 *arXiv:1708.02182 [cs]*, Aug. 2017.
- 472 [46] D. Neil, M. Pfeiffer, and S.-C. Liu. Phased LSTM: Accelerating Recurrent Network Training  
473 for Long or Event-based Sequences. *arXiv:1610.09513 [cs]*, Oct. 2016.
- 474 [47] D. Neil, J. H. Lee, T. Delbruck, and S.-C. Liu. Delta Networks for Optimized Recurrent Network  
475 Computation. In *International Conference on Machine Learning*, pages 2584–2593. PMLR,  
476 July 2017.
- 477 [48] C. Ostrau, C. Klarhorst, M. Thies, and U. Rückert. Benchmarking neuromorphic hardware and  
478 its energy expenditure. *Frontiers in Neuroscience*, page 732.
- 479 [49] N. Perez-Nieves and D. F. M. Goodman. Sparse Spiking Gradient Descent. *arXiv:2105.08810*  
480 *[cs, q-bio]*, May 2021.
- 481 [50] L. Pontryagin, V. Boltyanskiy, R. V. Gamkrelidze, and Y. MISHCHENKO. *Mathematical theory*  
482 *of optimal processes*. CRC press, 1962.

- 483 [51] O. Press and L. Wolf. Using the output embedding to improve language models. In *Proceedings*  
484 *of the 15th Conference of the European Chapter of the Association for Computational*  
485 *Linguistics: Volume 2, Short Papers*, pages 157–163, Valencia, Spain, Apr. 2017. Association  
486 for Computational Linguistics. URL <https://aclanthology.org/E17-2025>.
- 487 [52] A. Ramesh, M. Pavlov, G. Goh, S. Gray, C. Voss, A. Radford, M. Chen, and I. Sutskever.  
488 Zero-Shot Text-to-Image Generation. *arXiv:2102.12092 [cs]*, Feb. 2021.
- 489 [53] K. Roy, A. Jaiswal, and P. Panda. Towards spike-based machine intelligence with neuromorphic  
490 computing. *Nature*, 575(7784):607–617, 2019.
- 491 [54] T. K. Rusch and S. Mishra. Coupled Oscillatory Recurrent Neural Network (coRNN): An accurate  
492 and (gradient) stable architecture for learning long time dependencies. *arXiv:2010.00951 [cs,*  
493 *stat]*, Mar. 2021. URL <http://arxiv.org/abs/2010.00951>.
- 494 [55] D. Salaj, A. Subramoney, C. Krausnikovic, G. Bellec, R. Legenstein, and W. Maass. Spike  
495 frequency adaptation supports network computations on temporally dispersed information.  
496 *eLife*, 10:e65459, July 2021. ISSN 2050-084X. doi: 10.7554/eLife.65459. URL  
497 <https://doi.org/10.7554/eLife.65459>.
- 498 [56] S. Schaefer, D. Gehrig, and D. Scaramuzza. Aegnn: Asynchronous event-based graph neural  
499 networks. *arXiv preprint arXiv:2203.17149*, 2022.
- 500 [57] A. M. Schäfer and H. G. Zimmermann. Recurrent Neural Networks Are Universal Approximators.  
501 In S. D. Kollias, A. Stafylopatis, W. Duch, and E. Oja, editors, *Artificial Neural Networks –*  
502 *ICANN 2006*, Lecture Notes in Computer Science, pages 632–640, Berlin, Heidelberg, 2006.  
503 Springer. ISBN 978-3-540-38627-8. doi: 10.1007/11840817\_66.
- 504 [58] C. D. Schuman, T. E. Potok, R. M. Patton, J. D. Birdwell, M. E. Dean, G. S. Rose, and J. S.  
505 Plank. A survey of neuromorphic computing and neural networks in hardware. *arXiv preprint*  
506 *arXiv:1705.06963*, 2017.
- 507 [59] N. Shazeer, A. Mirhoseini, K. Maziarz, A. Davis, Q. Le, G. Hinton, and J. Dean. Outrageously  
508 Large Neural Networks: The Sparsely-Gated Mixture-of-Experts Layer. *arXiv:1701.06538*  
509 *[cs, stat]*, Jan. 2017.
- 510 [60] H. T. Siegelmann and E. D. Sontag. On the Computational Power of Neural Nets. *Journal*  
511 *of Computer and System Sciences*, 50(1):132–150, Feb. 1995. ISSN 0022-0000. doi:  
512 10.1006/jcss.1995.1013. URL [http://www.sciencedirect.com/science/article/pii/](http://www.sciencedirect.com/science/article/pii/S0022000085710136)  
513 [S0022000085710136](http://www.sciencedirect.com/science/article/pii/S0022000085710136).
- 514 [61] L. Wan, M. Zeiler, S. Zhang, Y. Le Cun, and R. Fergus. Regularization of neural networks  
515 using dropconnect. In S. Dasgupta and D. McAllester, editors, *Proceedings of the 30th*  
516 *International Conference on Machine Learning*, volume 28 of *Proceedings of Machine*  
517 *Learning Research*, pages 1058–1066, Atlanta, Georgia, USA, 17–19 Jun 2013. PMLR. URL  
518 <https://proceedings.mlr.press/v28/wan13.html>.
- 519 [62] J. Whittlestone, R. Nyrup, A. Alexandrova, K. Dihal, and S. Cave. Ethical and societal  
520 implications of algorithms, data, and artificial intelligence: a roadmap for research. *London:*  
521 *Nuffield Foundation*, 2019.
- 522 [63] T. C. Wunderlich and C. Pehle. Event-based backpropagation can compute exact gradients for spik-  
523 ing neural networks. *Scientific Reports*, 11(1):12829, June 2021. ISSN 2045-2322. doi: 10.1038/  
524 s41598-021-91786-z. URL <https://www.nature.com/articles/s41598-021-91786-z>.
- 525 [64] M. Yan, N. Meisburger, T. Medini, and A. Shrivastava. Distributed slide: Enabling training large  
526 neural networks on low bandwidth and simple cpu-clusters via model parallelism and sparsity.  
527 *arXiv preprint arXiv:2201.12667*, 2022.
- 528 [65] F. Zenke and S. Ganguli. SuperSpike: Supervised Learning in Multilayer Spiking Neural  
529 Networks. *Neural Computation*, 30(6):1514–1541, Apr. 2018. ISSN 0899-7667. doi:  
530 10.1162/neco\_a\_01086. URL [https://doi.org/10.1162/neco\\_a\\_01086](https://doi.org/10.1162/neco_a_01086).

531 **Checklist**

- 532 1. For all authors...
- 533 (a) Do the main claims made in the abstract and introduction accurately reflect the paper's  
534 contributions and scope? [Yes] See end of Section 1 for a summary of main claims.
- 535 (b) Did you describe the limitations of your work? [Yes] See Section 5.
- 536 (c) Did you discuss any potential negative societal impacts of your work? [Yes] See  
537 Section 5.
- 538 (d) Have you read the ethics review guidelines and ensured that your paper conforms to  
539 them? [Yes] The authors have read and approved the ethics guideline
- 540 2. If you are including theoretical results...
- 541 (a) Did you state the full set of assumptions of all theoretical results? [Yes] See Section 3  
542 and the Supplement
- 543 (b) Did you include complete proofs of all theoretical results? [Yes] See Section 3 and the  
544 Supplement
- 545 3. If you ran experiments...
- 546 (a) Did you include the code, data, and instructions needed to reproduce the main experimen-  
547 tal results (either in the supplemental material or as a URL)? [Yes] In the Supplement
- 548 (b) Did you specify all the training details (e.g., data splits, hyperparameters, how they were  
549 chosen)? [Yes] Some details in the main text and further details in Supplement
- 550 (c) Did you report error bars (e.g., with respect to the random seed after running experiments  
551 multiple times)? [Yes] In the Supplement
- 552 (d) Did you include the total amount of compute and the type of resources used (e.g., type  
553 of GPUs, internal cluster, or cloud provider)? [Yes] In the Supplement
- 554 4. If you are using existing assets (e.g., code, data, models) or curating/releasing new assets...
- 555 (a) If your work uses existing assets, did you cite the creators? [Yes]
- 556 (b) Did you mention the license of the assets? [Yes]
- 557 (c) Did you include any new assets either in the supplemental material or as a URL? [No]
- 558 (d) Did you discuss whether and how consent was obtained from people whose data you're  
559 using/curating? [N/A]
- 560 (e) Did you discuss whether the data you are using/curating contains personally identifiable  
561 information or offensive content? [N/A]
- 562 5. If you used crowdsourcing or conducted research with human subjects...
- 563 (a) Did you include the full text of instructions given to participants and screenshots, if  
564 applicable? [N/A]
- 565 (b) Did you describe any potential participant risks, with links to Institutional Review Board  
566 (IRB) approvals, if applicable? [N/A]
- 567 (c) Did you include the estimated hourly wage paid to participants and the total amount  
568 spent on participant compensation? [N/A]